JOURNAL OF VIROLOGY, May 2005, p. 6449–6458 Vol. 79, No. 10
0022-538X/05/$08.00+0 doi:10.1128/JVI.79.10.6449–6458.2005

Acylation-Mediated Membrane Anchoring of Avian Influenza Virus Hemagglutinin Is Essential for Fusion Pore Formation and Virus Infectivity

Ralf Wagner, Astrid Herwig, Nahid Azzouz, and Hans Dieter Klenk*

Institut für Virologie, Philipps-Universität, 35011 Marburg, Germany

Received 9 August 2004/Accepted 23 December 2004

Attachment of palmitic acid to cysteine residues is a common modification of viral glycoproteins. The influenza virus hemagglutinin (HA) has three conserved cysteine residues at its C terminus serving as acylation sites. To analyze the structural and functional roles of acylation, we have generated by reverse genetics a series of mutants (Ac1, Ac2, and Ac3) of fowl plague virus (FPV) containing HA in which the acylation sites at positions 551, 559, and 562, respectively, have been abolished. When virus growth in CV1 and MDCK cells was analyzed, similar amounts of virus particles were observed with the mutants and the wild type. Protein patterns and lipid compositions, characterized by high cholesterol and glycolipid contents, were also indistinguishable. However, compared to wild-type virus, Ac2 and Ac3 virions were 10 and almost 1,000 times less infectious, respectively. Fluorescence transfer experiments revealed that loss of acyl chains impeded formation of fusion pores, whereas hemifusion was not affected. When the affinity to detergent-insoluble glycolipid (DIG) domains was analyzed by Triton X-100 treatment of infected cells and virions, solubilization of Ac2 and Ac3 HAs was markedly facilitated. These observations show that acylation of the cytoplasmic tail, while not necessary for targeting to DIG domains, promotes the firm anchoring and retention of FPV HA in these domains. They also indicate that tight DIG association of FPV HA is essential for formation of fusion pores and thus probably for infectivity.

Influenza viruses are lipid-enveloped viruses with a genome consisting of eight segments of negative-stranded RNA. Two spike glycoproteins are found in the viral membrane, the hemagglutinin (HA) and the neuraminidase (NA). Both glycoproteins fulfill important functions during the viral replicative cycle (20). Virus infection is initiated by binding of HA to sialic acid-containing receptors on the surfaces of target cells. Following internalization of bound viruses by endocytosis, HA induces fusion of the viral envelope with the endosomal membrane (48). The fusion reaction proceeds via distinct steps, including the hemifusion intermediate (where the outer lipid leaflets of the two apposed membranes mix), the formation of a fusion pore, and finally the dilation of this pore (12, 14). This fusion event is an absolute requirement for the delivery of viral nucleocapsids into the cytoplasm of the infected cell and thus for the establishment of a productive infection.

HA, a class I transmembrane glycoprotein, is embedded in the lipid envelope as a homotrimer (56). Each monomer consists of a large ectodomain that carries receptor binding and fusion activities, a stretch of mainly hydrophobic amino acids which constitutes the transmembrane domain, and a short cytoplasmic tail. The cytoplasmic domain comprises 9 to 11 amino acids, depending on the HA subtype. Three cysteine residues in the C-terminal region, one in the transmembrane domain and two in the cytoplasmic tail, are extremely conserved throughout all HA subtypes analyzed to date (33). These cysteines are posttranslationally acylated by the addition of palmitic acids through thioester bonds (52), a modification commonly found on many other viral glycoproteins as well (38). The strict conservation of HA acylation sites suggests an important function of the protein-linked fatty acids in the viral life cycle. Some previous studies pointed towards a role in virus assembly, whereas others supported the notion that acylation is required for fusion.

Support for a role of acylation in assembly comes from reports revealing that H1, H2, and H7 HAs interact with specific membrane microdomains characterized by a high content of laterally associating glycosphingolipids and cholesterol (8, 41, 42, 45, 49). Due to their insolubility in nonionic detergents such as Triton X-100, these microdomains are termed detergent-insoluble glycolipid (DIG) domains. Since the glycoproteins of many other enveloped viruses are also found in these domains during assembly, it appears that DIG association might represent a general step in virus maturation (1, 4, 37, 53). While amino acid motifs within the H2 and H3 HA transmembrane domains seem to constitute the primary determinants for the interaction of HA with these compartments (3, 22, 42, 51), some evidence that protein-attached saturated fatty acids might also contribute to some extent to HA targeting into DIG domains has recently been obtained (28).

That palmitic acid residues are involved in the membrane fusion process was first suggested by studies showing that cells expressing deacylated HA of subtype H2 were unable to form syncytia (29). Syncytium formation is indicative of HA-driven fusion between neighboring cells. Restrictions in syncytium formation were also detected with acylation mutants of the fowl plague virus (FPV) HA (subtype H7) expressed in CV1

* Corresponding author. Mailing address: Institut für Virologie, Philipps-Universität Marburg, Postfach 2360, 35011 Marburg, Germany. Phone: 49 6421/28-66253. Fax: 49 6421/28-68962. E-mail: klenk@staff.uni-marburg.de.

cells (9). More recently, it was shown in a study employing vector-expressed H1 HA that acylation is required for the formation of aqueous fusion pores (40). However, studies with vector-expressed H3 HA failed to uncover any involvement of acyl chains in the fusion reaction (30, 47, 50), except for one report on fully deacylated H3 HA, which uncovered a contribution of fatty acids to fusion pore flickering (27). Moreover, using a reverse genetics approach, it was possible to recover infectious viral particles carrying H3 subtype HA from which all three acylation sites had been deleted (15). This suggested that fatty acids attached to H3 HA are essential neither for fusion nor for assembly. Interestingly, the situation was remarkably different with H1 HA. Here, no virus could be rescued when either of the two distally located acylation sites was deleted, but the question of whether acylation was required for particle formation or for fusion activity remained open (58).

In view of these seemingly controversial findings, we have established in the present study a reverse genetics system for the generation of FPV from cDNA to systematically study the role of HA acylation during virus replication. We show here that in the FPV system, loss of the acyl chains from the two distally located positions (mutants Ac2 and Ac3) interferes with the infectivity of the respective viruses by abrogating fusion pore formation. Deacylation disturbed neither targeting of HA to DIG domains nor budding of viruses from these domains. However, the two distally located acyl side chains were essential for the retention of HA within DIG domains, demonstrating that the firm anchoring of HA in these domains of the viral envelope is a prerequisite for the transition from hemifusion to pore formation and thus probably for virus infectivity.

MATERIALS AND METHODS

Cells and viruses. African green monkey kidney cells (CV1) and human embryonic kidney cells (293 cells) were maintained in Dulbecco's modified Eagle's medium (DMEM) supplemented with 5% (CV1 cells) or 10% (293 cells) fetal calf serum (FCS) (Invitrogen, Karlsruhe, Germany). Madin-Darby canine kidney (MDCK) cells were kept in minimal essential medium supplemented with 10% FCS. All cells were cultivated at 37°C with 5% CO_2. Plasmids for the generation of recombinant A/WSN/33 (H1N1) viruses were kindly provided by G. Neumann (Madison, Wisconsin).

Generation of recombinant viruses with acylation mutations. The virus A/FPV/Ro/34 (H7N1) was grown in 11-day-old embryonated chicken eggs. Virus was recovered from 1 ml of allantoic fluid by centrifugation at 120,000 × *g*, and viral RNA was isolated using the High Pure RNA isolation kit (Roche Molecular Biochemicals, Mannheim, Germany). Viral gene segments were transcribed into DNA and then amplified employing the OneStep reverse transcription-PCR (RT-PCR) kit (QIAGEN, Hilden, Germany). The following primers were used in the RT-PCR procedure: for the PB1 gene, 5′ATATACCTGCATAAGGGAGCGAAAGCAGGCA3′ (forward [fo]) and 5′ATATACCTGCATATTATTAGTAGAAACAAGGCA3′ (reverse [re]); for the PB2 gene, 5′ATATGGTCTCAGGGAGCGAAAGCAGGTC3′ (fo) and 5′ATATGGTCTCTTATTAGTAGAAACAAGGTC3′ (re); for the PA gene, 5′ATATGGTCTCAGGGAGCGAAAGCAGGTAC3′ (fo) and 5′ATATGGTCTCTTATTAGTAGAAACAAGGTAC3′ (re); for the HA gene, 5′ATATGGTCTCAGGGAGCAAAAGCAGGGGA3′ (fo) and 5′ATATGGTCTCTTATTAGTAGAAACAAGGGTGTTTTTTTC3′ (re); for the NP gene, 5′ATATACCTGCATAAGGGAGCAAAAGCAGGGTA3′ (fo) and 5′ATATACCTGCATATTATTAGTAGAAACAAGGGTA3′ (re); for the NA gene, 5′ATATGGTCTCAGGGAGCAAAAGCAGGAG3′ (fo) and 5′ATATGGTCTCCTTATTAGTAGAAACAAGGAGT3′ (re); for the M gene, 5′ATATCGTCTCAGGGAGCAAAAGCAGGTAG3′ (fo) and 5′ATATCGTCTCTTATTAGTAGAAACAAGGTAG3′ (re); and for the NS gene, 5′ATATCGTCTCAGGGAGCAAAAGCAGGGTG3′ (fo) and 5′ATATCGTCTCTTATTAGTAGAAACAAGGGTG3′ (re). These primers contained restriction endonuclease sites for either BspMI (PB1 and NP), BsaI (PB2, PA, HA, and NA), or BsmBI (M and NS). RT-PCR products were purified by preparative agarose gel electrophoresis and digested with the respective restriction enzymes to generate protruding termini. These fragments were then inserted into the plasmid pHH21 previously linearized with BsmBI (31). For rescue of recombinant FPV, 1 μg of each of these plasmids was transfected into 2×10^6 293T cells along with expression plasmids encoding the subunits of the influenza virus polymerase pcDNA-PB1 (1 μg), pcDNA-PB2 (1 μg), pcDNA-PA (0.2 μg), and pcDNA-NP (1 μg). The Lipofectamine 2000 transfection reagent (Invitrogen) was used according to the manufacturer's instructions. At 8 h posttransfection the medium was changed to DMEM containing 0.2% bovine serum albumin (BSA) and 0.5% FCS. At 2 days posttransfection the 293T cell supernatant was passaged onto MDCK cells to efficiently propagate recombinant viruses. To obtain chimeric viruses containing FPV HA in the background of the WSN virus, the rescue procedure was performed using the RNA polymerase I plasmid coding for FPV HA and seven residual plasmids coding for the gene segments of the strain A/WSN/33. Purification of rescued viruses was achieved by three plaque passages on MDCK cells.

FPV HA mutants were generated starting from the wild-type (WT) sequence present in the plasmid pHH21. To inactivate either of the three acylation sites, the respective cysteine residues were exchanged for serines by using the Quickchange mutagenesis kit (Stratagene, Amsterdam, The Netherlands). Primers used in this procedure were as follows: 5′GGCCTTGTTTTCATATCAGGTGAAGAACGGAAAC3′ (fo) and 5′GTTTCCGTTCTTCACTGATATGAAAACAAGGCC3′ (re) for exchange of cysteine at position 551, 5′GAACGGAAACATGCGATCGACTATTTGTATATAGG3′ (fo) and 5′CCTATATACAAATAGTCGATCGCATGTTTCCGTTC3′ (re) for exchange of cysteine at position 559, and 5′GGAAACATGCGGTGCACGATATCGATATAGGTTTGGAAAA3′ (fo) and 5′TTTTCCAAACCTATATCGATATCGTGCACCGCATGTTTCC3′ (re) for exchange of cysteine at position 562. The HA mutants were then employed for the generation of recombinant viruses as described above.

Replication of mutant viruses in cell culture. For growth curves, MDCK and CV1 cell monolayers were inoculated with viruses at a multiplicity of infection (MOI) of 0.001 in phosphate-buffered saline (PBS) containing 0.2% BSA for 1 h. Unbound viruses were washed away, and serum-free medium containing 0.2% BSA was added. From then on, HA titers in the supernatants were periodically monitored with chicken red blood cells (RBC) (1% in saline).

For plaque assays, confluent CV1 cell monolayers in 6-cm-diameter dishes were inoculated with 10-fold dilutions (in PBS–0.2% BSA) of mutant viruses for 1 h. Cells were then washed with PBS–0.2% BSA and covered with an overlay of DMEM containing 0.5% agar (Oxoid Ltd., Basingstoke, Hampshire, England), 0.2% BSA, and 0.001% DEAE-dextran. Plaques were stained at 3 days postinfection (p.i.) with 0.1% crystal violet in a 10% formaldehyde solution.

Purification of viral particles. CV1 cells (2×10^6) were inoculated at a high MOI with recombinant viruses in PBS–0.2% BSA for 1 h. To this end, inocula of sufficiently high titers had been prepared by propagation of virus mutants in the allantoic cavities of 11-day-old embryonated chicken eggs. Cells were washed and incubated in serum-free DMEM–0.2% BSA at 37°C for 16 h. Supernatants were harvested and cleared from cell debris by low-speed centrifugation. Virus particles were then pelleted by ultracentrifugation in a Beckman SW41 rotor for 4 h at 140,000 × *g* followed by velocity centrifugation on a sucrose step gradient (bottom, 60%; top, 20%) for 16 h at 120,000 × *g*. Viruses were collected from the gradient interface, again pelleted in a Beckman SW 41 rotor, and resuspended in PBS containing a protease inhibitor cocktail (Calbiochem, Bad Soden, Germany). Aliquots of these virus preparations were subjected to a 10% sodium dodecyl sulfate-polyacrylamide gel electrophoresis (SDS-PAGE), and proteins were blotted to nitrocellulose. Virus-specific proteins were detected with a polyclonal anti-FPV serum raised in rabbit.

Analysis of fusion activities. Hemifusion and pore formation activities were assayed using octadecyl rhodamine B (R18)- and calcein-labeled RBC, respectively. For labeling with R18, 5 ml of a freshly prepared guinea pig erythrocyte suspension (1% in PBS) was mixed with 3 μl R18 solution (4 mM in ethanol; Molecular Probes, Leiden, The Netherlands) and incubated for 30 min at room temperature in the dark on a rotary shaker. Next, 15 ml of DMEM with 10% FCS was added and incubation was continued for 20 min. For calcein labeling, 5 ml of the guinea pig RBC solution was mixed with 20 μl of calcein AM (10 mM in DMSO; Molecular Probes) and incubated for 1 h at 37°C in the dark. After incubation, the RBC from both labeling procedures were washed five times with PBS and resuspended in 20 ml of DMEM.

CV1 cell monolayers were infected at an MOI of approximately 0.25 with mutant viruses and incubated for 12 h. Cells were washed with PBS and overlaid with 1 ml each of the R18- and calcein-labeled RBC suspensions for 30 min on ice. Unbound RBC were washed off vigorously with PBS, and the fusion reaction was induced by transiently lowering the pH in the medium to 5.4 for 4 min at

37°C. The medium was then replaced by DMEM at neutral pH, and the progressions of hemifusion and pore formation were monitored in a fluorescence microscope with the rhodamine (510- to 560-nm excitation, 590-nm emission) and fluorescein isothiocyanate (450- to 490-nm excitation, 520-nm emission) filter sets, respectively.

Lipid analysis of viruses. Viruses were grown in large scale in CV1 cells and purified on a sucrose step gradient (see above) to obtain approximately 2 mg of viral protein. Lipids were isolated and analyzed as described previously (24). Briefly, lipids were extracted by adding chloroform-methanol (1:1, vol/vol) to the aqueous virus suspension to yield the final ratio of chloroform-methanol-water of 10:10:3 (vol/vol/vol), followed by extraction with chloroform-methanol-water (30:60:8, vol/vol/vol). Supernatants from both extractions were dried under nitrogen and redissolved in chloroform-methanol (1:1, vol/vol). Samples were applied to a DEAE-cellulose column and eluted with chloroform-methanol-water (30:60:8, vol/vol/vol) to obtain neutral lipids and subsequently with chloroform–methanol–0.8 M sodium acetate (30:60:8, vol/vol/vol) to release acidic lipids. Fractions were dried under nitrogen and desalted by partition between water and water-saturated *n*-butanol. The butanol phases were analyzed by thin-layer chromatography on Silica Gel 60 plates (Merck), using the solvent system chloroform–methanol–2 M NH_3 (65:25:4, vol/vol/vol). Standard mixtures containing individual lipid components were run alongside the samples (all lipid standards were obtained from Sigma, Taufkirchen, Germany). Plates were dried, sprayed with 3% cupric acetate–8% phosphoric acid solution, and heated to 180°C for 15 min to identify individual lipid components. Quantification was achieved by densitometric scanning of the thin-layer chromatography plates and comparison with lipid standards.

Analysis of DIG association of HA. CV1 cells (1×10^7) were infected at a high MOI with virus stocks obtained from allantoic fluids of embryonated chicken eggs and incubated for 14 h. Viruses were harvested and purified from the supernatants as described above. Infected cells and purified virions were then biotinylated. To this end, cells were washed twice with ice-cold PBS and treated three times with 5 ml biotin–*N*-hydroxysuccinimide (1 mg/ml in PBS; Calbiochem) for 10 min on ice. The reaction was stopped by adding 5 ml of 100 mM glycine in PBS for 10 min, and cells were washed twice with PBS, scraped off the dish, and collected by low-speed centrifugation. For biotinylation of virus, pellets were resuspended in 50 μl PBS and treated three times with 50 μl biotin (1 mg/ml in PBS) for 15 min on ice. The reaction was stopped with 100 μl 100 mM glycine in PBS for 10 min, and viruses were pelleted by centrifugation at 120,000 × *g*. Biotinylated samples were resuspended in either 500 μl (cells) or 100 μl (viruses) NTE buffer (25 mM Tris-HCl, 150 mM NaCl, 5 mM EDTA, pH 7.4) containing protease inhibitors and kept on ice. Triton X-100 was added to a final concentration of 1% (cells) and 0.1% (viruses), and samples were immediately mixed and kept on ice for 30 min. Triton X-100-soluble (supernatants) and -insoluble (pellets) fractions were separated by centrifugation at 120,000 × *g* for 2 h. Supernatants were adjusted to a volume of 500 μl with NTE buffer, and NP-40 and SDS were added to final concentrations of 1% and 0.2%, respectively. Triton-insoluble pellets were resuspended in 500 μl NTE buffer containing 1% Triton X-100, 1% NP-40, and 0.2% SDS by passing 20 times through a 0.4-mm needle. Biotinylated proteins from both fractions were precipitated by adding 40 μl of streptavidin (immobilized on agarose beads, 50% slurry in 0.02% sodium azide; Pierce, Bonn, Germany) and incubating overnight at 4°C with vigorous shaking. Beads were washed three times in NTE buffer containing 1% Triton X-100, 1% NP-40, and 0.1% SDS, and biotinylated proteins were eluted from the agarose beads by boiling in SDS-PAGE sample buffer for 10 min. Proteins were resolved by 10% SDS-PAGE, blotted to nitrocellulose, and detected with a polyclonal anti-FPV serum from rabbit.

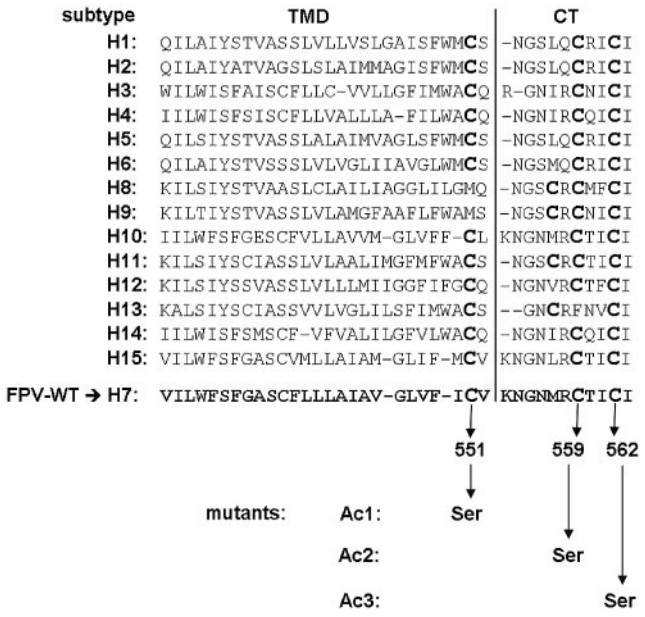

FIG. 1. Comparison of the carboxy-terminal amino acid sequences of 15 HA subtypes. Dashes are inserted to give maximum sequence homology. The conserved cysteine residues serving as acylation sites are shown in boldface. The FPV HA sequence is highlighted, and the nomenclature of the acylation mutants Ac1, Ac2, and Ac3, generated by exchanging cysteines for serines at positions 551, 559, and 562, respectively, is indicated. TMD, transmembrane domain; CT, cytoplasmic tail. The sequence alignment is adapted from that in reference 33. Strains and accession numbers of listed sequences are as follows: H1, A/PR/8/34, NC002017; H2, A/Japan/305/57, L20406; H3, A/Aichi/2/68, M55059; H4, A/duck/Czechoslovakia/56, M25283; H5, A/chicken/Pennsylvania/1370/83, M10243; H6, A/shearwater/Australia/1/72, D90303; H7, A/FPV/Rostock/34, M24457; H8, A/turkey/Ontario/6118/68, D90304; H9, A/turkey/Wisconsin/66, D90305; H10, A/chicken/Germany/N/49, M21647; H11, A/duck/England/56, D90306; H12, A/duck/Alberta/60/76, D90307; H13, A/gull/Maryland/704/77, D90308; H14, A/mallard/Gurjev/244/82, M35996; H15, A/shearwater/West-Australia/2576/79, L43917.

RESULTS

Generation and growth of recombinant FPV with acylation-deficient HA. Given the high conservation of acylation sites at the C terminus of HA, the aim of the present study was to elucidate the functional role of these fatty acids in virus replication. To this end, HA mutants Ac1, Ac2, and Ac3 were generated, in which the cysteines at positions 551, 559, and 562, respectively, were exchanged for serine in order to inactivate acylation sites (Fig. 1). Owing to the structural similarity of cysteine and serine, unintended effects of these amino acid exchanges other than abrogating acylation can be largely excluded. These HA mutants were then stably incorporated into recombinant FPV by applying a cDNA-based system that was originally developed for the generation of recombinant influenza viruses of the A/WSN/33 strain (31). Interestingly, recombinant FPV carrying HA in which more than one acylation site had been inactivated could not be rescued.

Virus growth was analyzed in CV1 and MDCK cells. Cultures were infected at a low multiplicity of infection of 0.001, and multiple-cycle replication was monitored by determining the HA titers in the culture supernatants over the next days (Fig. 2A). In neither CV1 nor MDCK cells did the loss of acylation from position 551 (mutant Ac1) have any effect on virus replication compared to WT viruses. However, when fatty acids were missing at position 559 or 562, replication efficiency was clearly reduced in both cell lines. These effects were somewhat more distinct in CV1 cells than in MDCK cells. Restriction in viral growth was much more pronounced in cells infected with Ac3 virus than in those infected with Ac2 virus. These data clearly demonstrate that the acyl side chain attached to HA at position 562 is an absolute requirement for efficient virus replication under multiple-cycle growth conditions, while that at position 559 is less important. No significant effect on replication could be attributed to the fatty acid linked

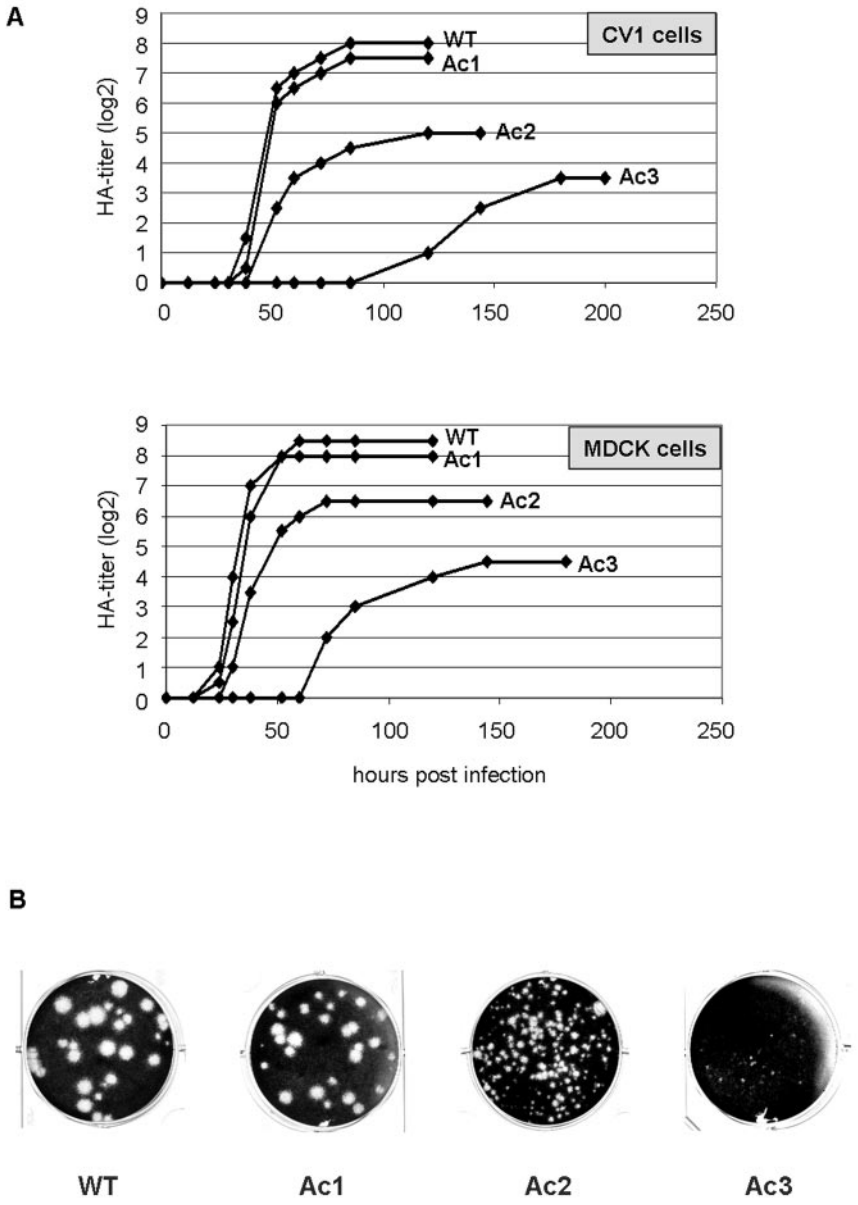

FIG. 2. Virus growth in cell culture. (A) Growth curves performed with CV1 and MDCK cells. Monolayers were inoculated at a low multiplicity of infection (0.001) and maintained at 37°C. Aliquots of supernatants were taken at the time points indicated and monitored for HA titers with chicken red blood cells. (B) Plaque formation. CV1 cell monolayers were inoculated with recombinant viruses and subsequently covered with an agarose-containing medium overlay. At 3 days postinfection, plaques were visualized by staining of monolayers with crystal violet.

to position 551. The situation was largely the same when virus spread was examined in CV1 cells by plaque assay (Fig. 2B). Here again, WT and Ac1 viruses produced plaques of roughly the same size, while only very tiny plaques were obtained with Ac3 virus and Ac2 virus showed an intermediate plaque size. Since the phenotype caused by deacylation was most evident in CV1 cells, these cells were used in all subsequent experiments.

Infectivity of viral particles. To analyze virus obtained under single-cycle growth conditions, we infected CV1 cells at high multiplicity and harvested culture supernatants 16 h p.i. Progeny virus was purified from the culture fluid by sucrose density gradient centrifugation, and protein profiles were subsequently analyzed by SDS-PAGE and Western blotting (Fig. 3A). In parallel, infectious titers in the supernatants were determined by plaque assay on CV1 cells. It is clear from the Western blot analysis that all four supernatants tested contained essentially the same amount of viral proteins, demonstrating that the lack of individual HA acyl side chains does not interfere with the production and release of virus particles. Likewise, the protein composition of all viruses released from CV1 cells was identical irrespective of HA acylation. Accordingly, acylation does not affect incorporation of HA into viral particles. However, there were striking differences in the infectivity of viral particles. We observed an almost 1,000-fold decline in infectivity of Ac3 virus compared to WT virus (Fig. 3B). The infectivity of Ac2 virus was reduced as well, albeit to a much lesser extent.

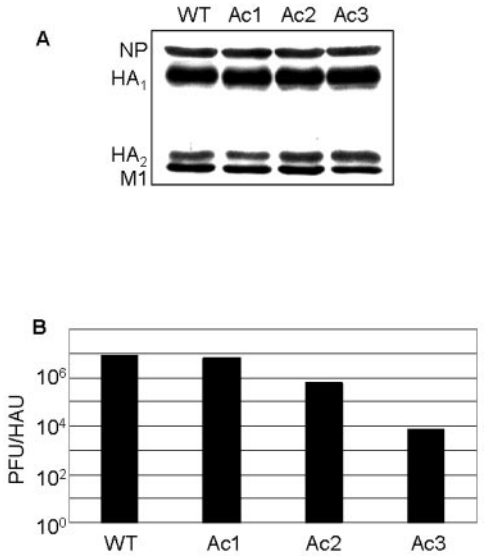

FIG. 3. Analysis of virus infectivity. (A) Protein composition of viral particles. CV1 cells were inoculated at a high multiplicity of infection, and culture supernatants were harvested at 16 h p.i. Progeny viruses were pelleted from the culture fluids by ultracentrifugation and subsequently purified by sucrose density step gradient centrifugation. Protein compositions of virus preparations were analyzed by reducing SDS-PAGE followed by Western blotting using an FPV-specific polyclonal antiserum. (B) Aliquots of the virus-containing CV1 culture supernatants were monitored for infectious titers by plaque assay on CV1 cell monolayers. HAU, hemagglutinination units.

Again, no such effect was seen with the Ac1 mutant. These results demonstrate that acylation of HA at position 562 is crucial for maintaining the infectivity of viral particles. The fatty acid attached to position 559 is less important, and that attached to cysteine residue 551 is not needed to render the virus infective. Thus, the restricted replication efficiencies seen with virus mutants Ac2 and Ac3 are probably due to the impairment of virus infectivity brought about by the lack of individual acyl chains.

Membrane fusion activity. The panel of recombinant viruses generated in this study has then been examined for fusion activity. Three different stages in HA-induced membrane fusion can be discriminated. In the first stage, the outer lipid leaflets of the viral envelope and the target membrane mix (hemifusion). Next, an aqueous pore is formed by connecting the inner leaflets of the lipid bilayers. Finally, there is dilation of the fusion pore. The abilities of HA mutants to induce the first two stages of the fusion reaction were examined in infected CV1 cells by using either R18- or calcein-labeled RBC from guinea pigs. To this end, cells were infected with virus mutants for 12 h, and labeled RBC were allowed to adhere to the surface of infected cells. The fusion reaction was induced by transiently lowering the pH to 5.4. Spread of the lipophilic stain R18 to the membrane of the underlying CV1 cells is indicative of hemifusion, while pore formation is evidenced by the transfer of the water-soluble dye calcein to the cytoplasm of the cells. We found that the loss of individual acyl side chains does not affect hemifusion. In all samples the fluorescent dye R18 passed on efficiently from the RBC to the plasma membrane, indicating that hemifusion proceeds with roughly the same kinetics irrespective of the acylation pattern of the viruses used for infection (Fig. 4). However, the situation turned out to be totally different for the next step of the fusion reaction, since loss of acylation from positions 559 and 562 drastically interfered with pore formation. All RBC-carrying cells infected with WT or Ac1 virus showed complete pore formation 30 min after acidification as revealed by the efficient transfer of calcein into the cytoplasm (Fig. 4). In contrast, at that time uptake of calcein was detected in only very few CV1 cells infected with Ac2 and Ac3 mutant viruses. The number of pore formation-positive cells did not increase during the next 2 h (data not shown). Restriction of pore formation was slightly more pronounced in cells infected with Ac3 virus than in those infected with Ac2 virus. Thus, whereas fatty acids attached to HA are dispensable for hemifusion, those attached to positions 559 and 562 are strictly needed for efficient fusion pore formation. Formation of an aqueous pore between the viral envelope and the endosome is an absolute requirement for viral ribonucleoproteins to gain access to the cytoplasm of the infected cell and thus for the establishment of infection. Hence, the reduced pore formation activities most probably account for the loss of infectivity seen with Ac2 and Ac3 viruses. Deacylation has no effect on transport and surface expression of HA (9, 27, 50). Hence, it is unlikely that the differences in pore formation are due to variations in HA surface densities.

Lipid composition of viral envelopes. HA localizes to DIG domains in the plasma membrane of infected cells (42). The observation that many DIG-resident proteins carry saturated fatty acids led to the idea that acylation might contribute to the DIG association of proteins (28). This potential involvement of protein-bound acyl side chains in the interaction with lipid microdomains prompted us to have a closer look at the lipid compositions of our virus mutants. To this end, lipids were extracted from purified virus obtained from CV1 cells, separated by thin-layer chromatography, and quantified by densitometric analysis (Table 1). There was a marked enrichment of DIG-resident glycosphingolipids, mainly ganglioside GM1, and cholesterol in both mutant and WT viruses compared to membranes of uninfected CV1 cells, but there were no differences between virus species. This indicates that the loss of acylation does not affect the lipid composition of the viral envelope. Taken together, our data show that neither the protein nor the lipid composition of virus particles is affected by the acylation pattern of HA. Accordingly, it can be concluded that irrespective of the presence of individual acyl side chains, the HA protein is targeted to DIG domains and is incorporated into progeny virus in association with these microdomains.

DIG association of HA. We then examined the extractability of HA mutants from the DIG domains by treatment with Triton X-100. Viruses were harvested from infected CV1 cells and purified on sucrose density gradients. After biotinylation, proteins expressed on the surfaces of infected cells and of purified viruses were treated with Triton X-100. HAs from infected cells and purified viruses responded very differently to treatment with Triton X-100. Viral HA was more detergent sensitive than that from infected cells, as has already been observed before by others (57). Consequently, for our studies we used 1% Triton X-100 when assaying DIG association of HA in infected cells and only 0.1% Triton X-100 when ana-

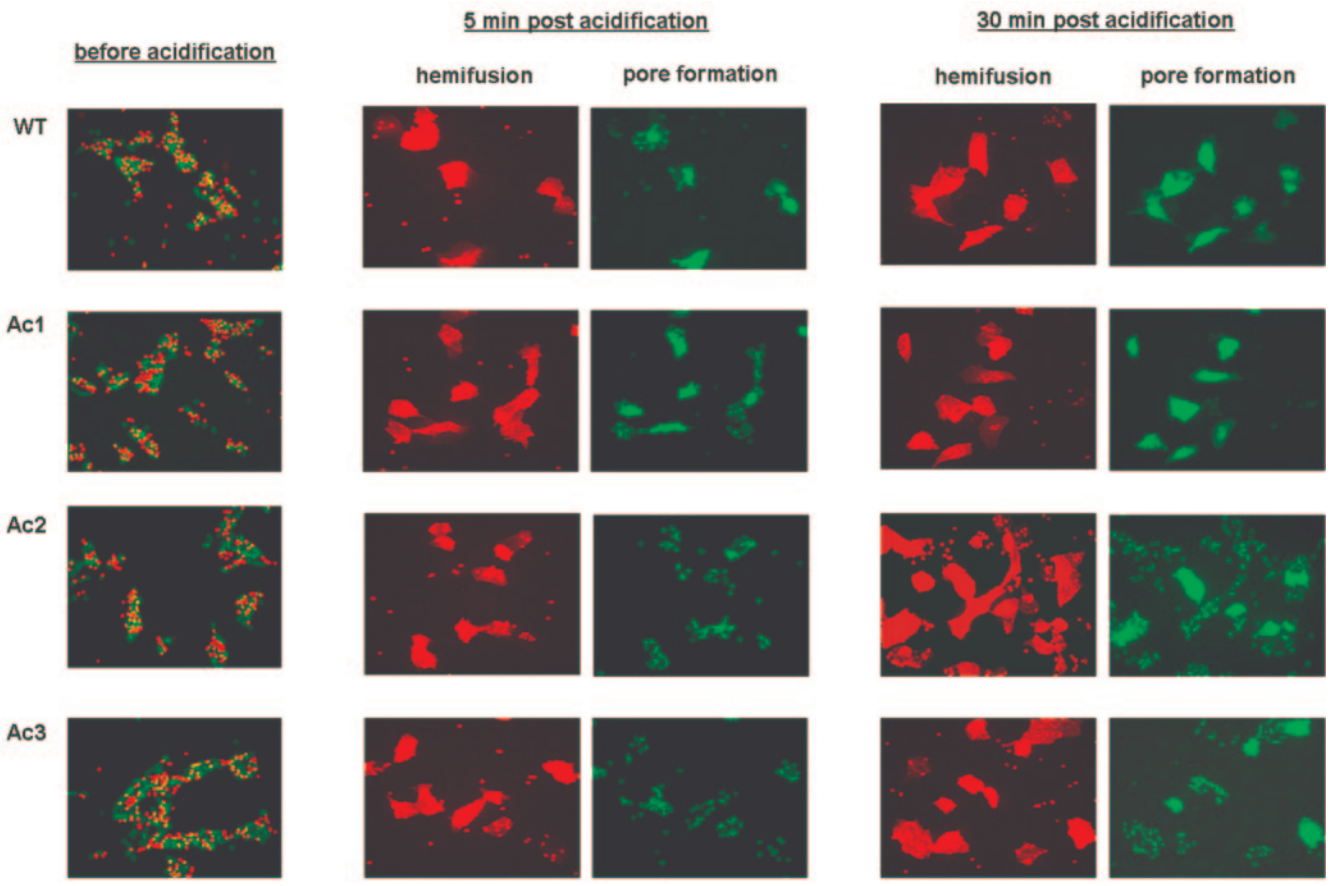

FIG. 4. Analysis of hemifusion and fusion pore formation in infected CV1 cells. Cells were inoculated at an MOI of about 0.25. At 12 h p.i., R18- and calcein-labeled RBC were adsorbed to HA expressed on the cell surface (i.e., before acidification). Fusion was triggered by transiently shifting the pH to 5.4. Hemifusion and fusion pore formation are revealed by the transition of R18 (red fluorescence) and calcein (green fluorescence) labels into membranes and into the cytoplasm of the underlying cells, respectively. Progression of the fusion process was monitored in the fluorescence microscope at 5 min and 30 min postacidification.

lyzing purified viruses. Detergent-soluble and insoluble fractions were separated by ultracentrifugation, and biotinylated proteins from both fractions were collected (Fig. 5). We found that the two acyl side chains attached next to the carboxy terminus are crucial for the stable association of HA with DIG domains. While hardly any difference in the response to detergent treatment was seen with WT and Ac1 viruses, HA solubilization was significantly increased with mutants Ac2 and Ac3. WT HA was retained almost completely in DIG domains in infected cells as well as in virus particles. Yet, more than 30% of Ac2 HA and 70% of Ac3 HA could be extracted by this treatment. Thus, fatty acids attached at positions 559 and 562 are essential to tightly anchor the HA protein within specialized lipid microdomains.

Interestingly, taking into account the data obtained on viral infectivity, it appeared that the tightness of HA DIG association and the infectivity of the respective viruses seem to be correlated. This observation was further corroborated by testing a different set of virus mutants. To this end, we generated chimeric recombinant viruses in which the FPV HA mutants were incorporated into the background of the virus strain A/WSN/33. As seen before for fully recombinant FPV, also in

TABLE 1. Lipid compositions of CV1 cells and recombinant viruses grown in these cells

Lipid	μg/mg of viral protein (mean ± SD)				
	WT virus	Ac1	Ac2	Ac3	CV1 cells
Phosphatidylethanolamine	71.6 ± 15.9	67.6 ± 12.9	75.6 ± 11.1	74.0 ± 10.7	47.8 ± 6.2
Phosphatidylcholine	69.2 ± 13.8	64.8 ± 12.6	73.3 ± 8.7	71.2 ± 10.5	83.2 ± 16.1
Cerebroside[a]	44.9 ± 7.5	41.8 ± 7.7	51.4 ± 9.3	54.9 ± 9.0	17.7 ± 3.9
Sphingomyelin[a]	38.0 ± 8.1	36.2 ± 5.7	40.4 ± 6.8	43.9 ± 4.5	9.6 ± 2.8
Cholesterol[a]	70.8 ± 7.3	62.8 ± 5.9	67.6 ± 5.4	71.4 ± 6.2	28.1 ± 3.5
Ganglioside GM1[a]	5.2 ± 1.2	4.8 ± 1.3	5.1 ± 1.6	5.3 ± 1.4	0.5 ± 0.2

[a] DIG-resident component.

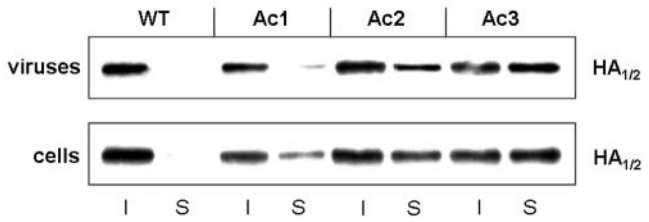

FIG. 5. Analysis of the detergent extractability of mutant HAs from membranes of infected CV1 cells and budded virions. FPV recombinants were harvested from culture supernatants and purified by sucrose density step gradient centrifugation. Infected cell monolayers and virus preparations were surface biotinylated and subsequently treated on ice with either 1% Triton X-100 (cells) or 0.1% Triton X-100 (viruses). Detergent-insoluble (I) and soluble (S) fractions were separated by ultracentrifugation, and biotinylated proteins from both fractions were precipitated using streptavidin-agarose beads. Next, the precipitated proteins were analyzed by SDS-PAGE under nonreducing conditions followed by Western blotting using an FPV-specific polyclonal antiserum. Only the $HA_{1/2}$ protein band is depicted.

this system the ease of extractability of HA corresponds to the decrease in viral infectivity (Fig. 6).

DISCUSSION

Palmitoylation of the cytoplasmic tail is a highly conserved trait of influenza virus HA (33, 52). To analyze the biological role of this modification, we have established a helper virus-free reverse genetics system for the generation of recombinant FPV carrying mutant HAs in which either of the three acylation sites had been inactivated by exchanging individual cysteine residues for serine residues. Our results show that, depending on the deleted acylation site, there is a decrease in the growth rates of the mutants when cells are infected under conditions of multiple-cycle replication. While barely any effect was detectable with mutant Ac1, lacking the fatty acid at position 551, it was quite distinct with mutants Ac2 and Ac3, lacking cysteines 559 and 562, respectively. It is of interest in this context that attempts to generate acylation mutants by replacing the cysteines at the second and the third positions by serines have not been successful when a helper virus-dependent system was used. Rescue of replication-competent virus occurred only when amino acids of higher hydrophobicity, such as tyrosine or phenylalanine, were introduced instead of cysteine (58). This illustrates the high efficiency of our helper-independent system for the production of virus mutants which in the past could not be generated. These earlier results along with our data depicted here strongly point to the requirement of hydrophobic constituents in the cytoplasmic tail of HA to allow for efficient virus growth. The crucial impact of FPV HA acylation on virus replication is also reflected by the observation that even with our system we were unable to rescue double or triple mutants of FPV lacking more than one acyl side chain (data not shown). In view of these results, it was of great interest to investigate at which step in the replication cycle HA fatty acids exert their function.

Comparison of viral particle yields and plaque-forming abilities of culture supernatants of infected CV1 cells revealed a marked decrease in the infectivities of Ac2 and Ac3 mutants. Although all viruses were released from cells with basically the same efficiency, Ac3 mutants suffered from an almost 1,000-fold decline in infectivity, which is in line with the replication properties observed before. Hence, the vast majority of Ac3 virus appears to be noninfectious, indicating that acylation at position 562 is crucial for infectivity. It has to be pointed out that WT and mutant particles were morphologically indistinguishable when analyzed in the electron microscope (data not shown). It is also noteworthy that there were no differences in protein and lipid compositions of virions. These observations indicate that the decrease in infectivity cannot be attributed to aberrant virus assembly. In particular, there was no evidence that deacylation interfered with FPV HA incorporation into virus particles. This observation is in agreement with previous findings indicating that fatty acids do not affect the rate of intracellular transport and cell surface expression of HA of different subtypes (9, 30, 47).

Covalently attached saturated fatty acids have been implicated in contributing to the association of the respective protein with DIG domains (28, 44). These are laterally organized lipid microdomains containing large amounts of sphingolipids and cholesterol. They serve as selective concentration devices for particular proteins and provide a platform for signal transduction (6, 43, 45, 46). Not only does influenza virus HA associate with DIG domains (8, 49), but these domains are also incorporated into virions during the assembly process (3, 41, 51, 57). It has long been known that viral membranes are rich

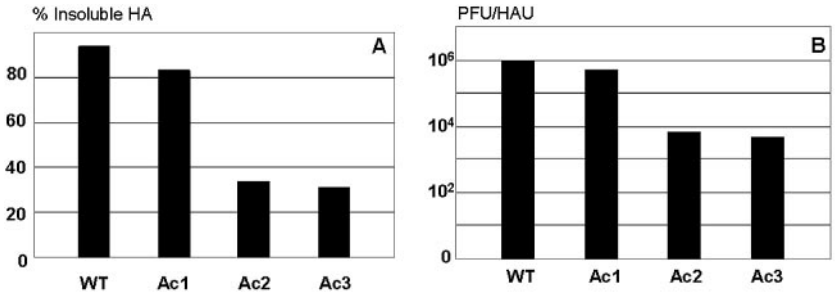

FIG. 6. Correlation of tightness of HA anchoring in DIG domains and virus infectivity in chimeric viruses containing the FPV HA in the background of the influenza virus A/WSN/33. (A) DIG association of HA in virus mutants was determined as outlined in the legend to Fig. 5. Bars represent the amount of Triton X-100-insoluble HA in relation to total HA. (B) Infectious titers of viruses grown in CV1 cells. Cells were inoculated at a high MOI with virus mutants, and supernatants harvested after 16 h were assayed for infectious progeny viruses by plaque assay on CV1 cells. Titers are expressed on the basis of the hemagglutinating units detected in culture supernatants. HAU, hemagglutinination units.

in cholesterol (17), and from numerous studies on other enveloped viruses, such as measles virus (25), Ebola and Marburg viruses (4), Newcastle disease virus (7), respiratory syncytial virus (5), and Sendai virus (1), strong evidence has emerged that DIG association of glycoproteins represents a common phenomenon in viral particle maturation. In particular, quite a comprehensive picture on the contribution of DIG domains to the biology of retroviruses has evolved in recent years. It was shown that covalently bound lipids promote the association of the viral Gag and envelope proteins with DIG domains of the plasma membrane (21, 39) and that this association plays a critical role not only for the assembly and release of virus particles (23, 32, 37), but also for virus entry into the host cell (10).

In the light of these observations, we were surprised to find that deacylation of FPV HA does not affect the lipid composition of the viral envelope. Most significantly, glycosphingolipids and cholesterol were markedly enriched in the envelopes of all WT as well as mutant viruses compared to the membranes of the CV1 host cells. These findings, along with identical amounts of proteins found in all viruses, clearly reveal that acylation-mutant HA resides in DIG domains and is incorporated into virions during budding from these domains in the same way as WT HA. Yet, a clear difference emerged when detergent extractability of HA from membranes was assayed. Ac3 HA and, to a lesser extent, also Ac2 HA were easily extracted with Triton X-100, while WT and Ac1 HAs were almost completely resistant to such treatment. Accordingly, the fatty acids attached to cysteines 562 and 559 are essential to tightly anchor the FPV HA molecule in the viral envelope. Takeda and coworkers (51) reported recently that amino acid exchanges in the transmembrane domain of HA of the Udorn strain (subtype H3) caused reduced DIG association. Unlike deacylation of the cytoplasmic tail, however, these mutations resulted in virus particles with decreased amounts of HA, supporting the concept that hydrophobic residues in the transmembrane domain constitute the primary motif mediating targeting to cholesterol-glycosphingolipid domains (3, 42). Taken together, the data show that acylation of the cytoplasmic tail enforces the tight anchoring and retention of FPV HA in cholesterol-glycosphingolipid domains, whereas the transmembrane sequence contains the targeting signal.

Mediating membrane fusion is a prime function of HA in the infection process (48). Upon analysis of discrete steps of the fusion reaction in CV1 cells infected with virus mutants, it became clear that hemifusion was not affected by the loss of individual acyl side chains of FPV HA. However, pore formation was severely reduced in Ac3-infected cells and, to a slightly lesser extent, in Ac2-infected cells. Given the importance of the fusion pore for the delivery of ribonucleoproteins into the infected cell, it is fair to conclude that the reduction in pore formation accounts for the reduction in infectivity of Ac2 and Ac3 viruses. However, there is no quantitative correlation between the extent of restriction of fusion pore formation and the observed infectivity of Ac2 and Ac3 viruses. This might be due to differences in the ability of these HA mutants to promote pore dilation. This late step of the fusion reaction, which is essential for the delivery of viral nucleocapsids into the host cell and thus for the establishment of a productive infection, has not been analyzed in this study. Moreover, it is conceivable that the data obtained in the fusion assay employing an artificial fluorescent substrate cannot be correlated one to one with those for virus infectivity.

It has to be pointed out that acylation may have diverse effects with different viruses. Such differences have been observed, for instance, between influenza viruses and retroviruses. When acylation of the envelope glycoproteins of retroviruses was abolished, surface transport and incorporation into virions were reduced with a concomitant loss in infectivity (21, 34, 39). On the other hand, there is no evidence that acylation affects the fusion property of the retrovirus envelope glycoprotein, again in contrast to the case for influenza virus HAs of subtypes H1, H2, and H7. Such differences may depend on the structure of the cytoplasmic tail of the transmembrane proteins, which is much bigger with Env than with HA.

As pointed out in the introduction, even within the influenza viruses there are controversial findings on the role of acylation. Some of these discrepancies have been resolved with increasing insight into the mechanisms of virus replication. Thus, we reported in one of the early studies on HA acylation that this modification has no effect on fusion activity of subtype H7 (52). However, when it was recognized that H7 HA required coexpression of M2 for structural integrity, it became clear that the fusion activity of this hemagglutinin depended on acylation (9, 36), as is also the case with subtypes H1 and H2 (29, 40, 58). The only exception is H3 HA, where such an effect has not been observed, regardless of whether the hemagglutinin was expressed alone (27, 47, 50) or as recombinant virus (15, 47). It has to be pointed out, however, that H3 HA was reassorted in the recombinants with heterologous genes of the WSN strain. It is therefore conceivable that acylation dependence of H3 HA fusion is detected only if this hemagglutinin is expressed in the context of homologous viral proteins, such as homologous M1 and/or M2 as in the case of H7 HA. In the present work a reduction in pore formation activity due to deacylation at individual sites was evident. No such effect was detected in a study by Fischer and coworkers on expressed HA (9). Again, the lack of residual viral proteins is likely to account for these differences.

Why does acylation of FPV HA promote pore formation? An important role of the transmembrane domain and the cytoplasmic tail in the fusion process was proposed a few years ago in a study employing glycosylphosphatidylinositol-anchored HA. This HA, which is anchored only in the outer leaflet of the membrane, proved capable of inducing hemifusion but failed to mediate complete fusion with the opening and dilation of a fusion pore (16). Other studies supported the concept that the transmembrane and the cytoplasmic portions of HA are crucial for the formation and enlargement of the fusion pore (2, 18, 26, 35). From our results it is obvious that fatty acids attached to the cytoplasmic tail represent important structural determinants ruling the infectivity of influenza viruses by specifically promoting the transition from hemifusion to pore formation. In order to induce fusion, the HA protein has to undergo extensive molecular rearrangements (13, 48, 54, 55). After exposure to low pH, the HA molecule initially adopts an extended conformation with the fusion peptide inserted in the endosomal membrane and the transmembrane and cytoplasmic domains anchored in the viral envelope. HA then undergoes a series of additional conformational changes,

finally resulting in the formation of a highly stable hairpin-like structure in which the fusion peptide and the transmembrane and cytoplasmic domains are relocated to the same end of the molecule. At the same time, this protein refolding also pulls the two apposed membranes towards each other to bring on fusion of the lipid bilayers (14). First, the outer leaflets of the two membranes merge, forming a hemifusion stalk (19). For a fusion pore to develop, the inner leaflets also have to mix. Therefore, these inner leaflets need to be forced into very close contact, which is accomplished by the free energy released during the folding of HA into its most stable conformation. Merging of the inner leaflets appears to be specifically exerted by the transmembrane domain and the cytoplasmic tail, as suggested by the observation that the fusion peptide is unlikely to penetrate into the inner leaflet of the target membrane (11). This scenario could explain the strict requirement of acyl side chains for pore formation. By enhancing the hydrophobic interactions of the cytoplasmic tail with the inner lipid leaflet, acyl side chains, in conjunction with cholesterol-glycolipid microdomains, tightly fix the HA C terminus to this membrane layer. This then allows for the force from protein refolding to be transformed into the movement of membranes. According to this model, any lack of such a tight anchoring of HA within the inner lipid layer brought about by either shortening the transmembrane domain, anchoring by a glycosylphosphatidylinositol anchor, or loss of acylation would drastically reduce pore formation.

ACKNOWLEDGMENTS

We are grateful to Gabriele Neumann for kindly providing the set of plasmids for the generation of the influenza A/WSN/33 virus.

This work was supported by grants from the Deutsche Forschungsgemeinschaft (SFB 593) and from Fonds der Chemischen Industrie.

REFERENCES

1. **Ali, A., and D. P. Nayak.** 2000. Assembly of Sendai virus: M protein interacts with F and HN proteins and with the cytoplasmic tail and transmembrane domain of F protein. Virology **276:**289–303.
2. **Armstrong, R. T., A. S. Kushnir, and J. M. White.** 2000. The transmembrane domain of influenza hemagglutinin exhibits a stringent length requirement to support the hemifusion to fusion transition. J. Cell Biol. **151:**425–437.
3. **Barman, S., A. Ali, E. K. Hui, L. Adhikary, and D. P. Nayak.** 2001. Transport of viral proteins to the apical membranes and interaction of matrix protein with glycoproteins in the assembly of influenza viruses. Virus Res. **77:**61–69.
4. **Bavari, S., C. M. Bosio, E. Wiegand, G. Ruthel, A. B. Will, T. W. Geisbert, M. Hevey, C. Schmaljohn, A. Schmaljohn, and M. J. Aman.** 2002. Lipid raft microdomains: a gateway for compartmentalized trafficking of Ebola and Marburg viruses. J. Exp. Med. **195:**593–602.
5. **Brown, G., H. W. Rixon, and R. J. Sugrue.** 2002. Respiratory syncytial virus assembly occurs in GM1-rich regions of the host-cell membrane and alters the cellular distribution of tyrosine phosphorylated caveolin-1. J. Gen. Virol. **83:**1841–1850.
6. **Cary, L. A., and J. A. Cooper.** 2000. Molecular switches in lipid rafts. Nature **404:**945–947.
7. **Dolganiuc, V., L. McGinnes, E. J. Luna, and T. G. Morrison.** 2003. Role of the cytoplasmic domain of the Newcastle disease virus fusion protein in association with lipid rafts. J. Virol. **77:**12968–12979.
8. **Fiedler, K., T. Kobayashi, T. V. Kurzchalia, and K. Simons.** 1993. Glycosphingolipid-enriched, detergent-insoluble complexes in protein sorting in epithelial cells. Biochemistry **32:**6365–6373.
9. **Fischer, C., B. Schroth-Diez, A. Herrmann, W. Garten, and H. D. Klenk.** 1998. Acylation of the influenza hemagglutinin modulates fusion activity. Virology **248:**284–294.
10. **Guyadar, M., E. Kiyokawa, L. Abrami, P. Turelli, and D. Trono.** 2002. Role for human immunodeficiency virus type 1 membrane cholesterol in viral internalization. J. Virol. **76:**10356–10364.
11. **Han, X., J. H. Bushweller, D. S. Cafiso, and L. K. Tamm.** 2001. Membrane structure and fusion-triggering conformational change of the fusion domain from influenza hemagglutinin. Nat. Struct. Biol. **8:**715–720.
12. **Hernandez, L. D., L. R. Hoffman, T. G. Wolfsberg, and J. M. White.** 1996. Virus-cell and cell-cell fusion. Annu. Rev. Cell Dev. Biol. **12:**627–661.
13. **Hughson, F. M.** 1995. Structural characterization of viral fusion proteins. Curr. Biol. **5:**265–274.
14. **Jardetzky, T. S., and R. A. Lamb.** 2004. Virology: a class act. Nature **427:** 307–308.
15. **Jin, H., K. Subbarao, S. Bagai, G. P. Leser, B. R. Murphy, and R. A. Lamb.** 1996. Palmitylation of the influenza virus hemagglutinin (H3) is not essential for virus assembly or infectivity. J. Virol. **70:**1406–1414.
16. **Kemble, G. W., T. Danieli, and J. M. White.** 1994. Lipid-anchored influenza hemagglutinin promotes hemifusion, not complete fusion. Cell **76:**383–391.
17. **Klenk, H. D., and P. W. Choppin.** 1970. Plasma membrane lipids and parainfluenza virus assembly. Virology **40**:939–947.
18. **Kozerski, C., E. Ponimaskin, B. Schroth-Diez, M. F. Schmidt, and A. Herrmann.** 2000. Modification of the cytoplasmic domain of influenza virus hemagglutinin affects enlargement of the fusion pore. J. Virol. **74:**7529–7537.
19. **Kuzmin, P. I., J. Zimmerberg, Y. A. Chizmadzhev, and F. S. Cohen.** 2001. A quantitative model for membrane fusion based on low-energy intermediates. Proc. Natl. Acad. Sci. USA **98:**7235–7240.
20. **Lamb, R. A., and R. M. Krug.** 2001. Orthomyxoviridae: the viruses and their replication, p. 1487–1531. *In* B. N. Fields, D. M. Knipe, and P. M. Howley (ed.), Fields virology. Lippincott Williams & Wilkins, Philadelphia, Pa.
21. **Li, M., C. Yang, S. Tong, A. Weidmann, and R. W. Compans.** 2002. Palmitoylation of the murine leukemia virus envelope protein is critical for lipid raft association and surface expression. J. Virol. **76:**11845–11852.
22. **Lin, S., H. Y. Naim, A. C. Rodriguez, and M. G. Roth.** 1998. Mutations in the middle of the transmembrane domain reverse the polarity of transport of the influenza virus hemagglutinin in MDCK epithelial cells. J. Cell Biol. **142:**51–57.
23. **Lindwasser, O. W., and M. D. Resh.** 2001. Multimerization of human immunodeficiency virus type 1 Gag promotes its localization to barges, raft-like membrane microdomains. J. Virol. **75:**7913–7924.
24. **Macala, L. J., R. K. Yu, and S. Ando.** 1983. Analysis of brain lipids by high performance thin-layer chromatography and densitometry. J. Lipid Res. **24:**1243–1250.
25. **Manie, S. N., S. Debreyne, S. Vincent, and D. Gerlier.** 2000. Measles virus structural components are enriched into lipid raft microdomains: a potential cellular location for virus assembly. J. Virol. **74:**305–311.
26. **Melikyan, G. B., S. Lin, M. G. Roth, and F. S. Cohen.** 1999. Amino acid sequence requirements of the transmembrane and cytoplasmic domains of influenza virus hemagglutinin for viable membrane fusion. Mol. Biol. Cell **10:**1821–1836.
27. **Melikyan, G. B., H. Jin, R. A. Lamb, and F. S. Cohen.** 1997. The role of the cytoplasmic tail of influenza virus hemagglutinin in formation and growth of fusion pores. Virology **235:**118–128.
28. **Melkonian, K. A., A. G. Ostermeyer, J. Z. Chen, M. G. Roth, and D. A. Brown.** 1999. Role of lipid modifications in targeting proteins to detergent-resistant membrane rafts. Many raft proteins are acylated, while few are prenylated. J. Biol. Chem. **274:**3910–3917.
29. **Naeve, C. W., and D. Williams.** 1990. Fatty acids on the A/Japan/305/57 influenza virus hemagglutinin have a role in membrane fusion. EMBO J. **9:**3857–3866.
30. **Naim, H. Y., B. Amarneh, N. T. Ktistakis, and M. G. Roth.** 1992. Effects of altering palmitylation sites on biosynthesis and function of the influenza virus hemagglutinin. J. Virol. **66:**7585–7588.
31. **Neumann, G., T. Watanabe, H. Ito, S. Watanabe, H. Goto, P. Gao, M. Hughes, D. R. Perez, R. Donis, E. Hoffmann, G. Hobom, and Y. Kawaoka.** 1999. Generation of influenza A viruses entirely from cloned cDNAs. Proc. Natl. Acad. Sci. USA **96:**9345–9350.
32. **Nguyen, D. H., and J. E. K. Hildreth.** 2000. Evidence for budding of human immunodeficiency virus type 1 selectively from glycolipid-enriched membrane lipid rafts. J. Virol. **74:**3264–3272.
33. **Nobusawa, E., T. Aoyama, H. Kato, Y. Suzuki, Y. Tateno, and K. Nakajima.** 1991. Comparison of complete amino acid sequences and receptor-binding properties among 13 serotypes of hemagglutinins of influenza A viruses. Virology **182:**475–485.
34. **Ochsenbauer-Jambor, C., D. C. Miller, C. R. Roberts, S. S. Rhee, and E. Hunter.** 2001. Palmitoylation of the rous sarcoma virus transmembrane glycoprotein is required for protein stability and virus infectivity. J. Virol. **75:**11544–11554.
35. **Ohuchi, M., C. Fischer, R. Ohuchi, A. Herwig, and H. D. Klenk.** 1998. Elongation of the cytoplasmic tail interferes with the fusion activity of influenza virus hemagglutinin. J. Virol. **72:**3554–3559.
36. **Ohuchi, M., A. Cramer, M. Vey, R. Ohuchi, W. Garten, and H.-D. Klenk.** 1994. Rescue of vector-expressed fowl plague virus hemagglutinin in biologically active form by acidotropic agents and coexpressed M2 protein. J. Virol. **68:**920–926.
37. **Ono, A., and E. O. Freed.** 2001. Plasma membrane rafts play a critical role in HIV-1 assembly and release. Proc. Natl. Acad. Sci. USA **98:**13925–13930.
38. **Resh, M. D.** 1999. Fatty acylation of proteins: new insights into membrane targeting of myristoylated and palmitoylated proteins. Biochim. Biophys. Acta **1451:**1–16.
39. **Rousso, I., M. B. Mixon, B. K. Chen, and P. S. Kim.** 2000. Palmitoylation of

the HIV-1 envelope glycoprotein is critical for viral infectivity. Proc. Natl. Acad. Sci. USA **97:**13523–13525.
40. **Sakai, T., R. Ohuchi, and M. Ohuchi.** 2002. Fatty acids on the A/USSR/77 influenza virus hemagglutinin facilitate the transition from hemifusion to fusion pore formation. J. Virol. **76:**4603–4611.
41. **Scheiffele, P., A. Rietveld, T. Wilk, and K. Simons.** 1999. Influenza viruses select ordered lipid domains during budding from the plasma membrane. J. Biol. Chem. **274:**2038–2044.
42. **Scheiffele, P., M. G. Roth, and K. Simons.** 1997. Interaction of influenza virus haemagglutinin with sphingolipid-cholesterol membrane domains via its transmembrane domain. EMBO J. **16:**5501–5508.
43. **Schroeder, F., A. M. Gallegos, B. P. Atshaves, S. M. Storey, A. L. McIntosh, A. D. Petrescu, H. Huang, O. Starodub, H. Chao, H. Yang, A. Frolov, and A. B. Kier.** 2001. Recent advances in membrane microdomains: rafts, caveolae, and intracellular cholesterol trafficking. Exp. Biol. Med. **226:**873–890.
44. **Schroeder, R., E. London, and D. Brown.** 1994. Interactions between saturated acyl chains confer detergent resistance on lipids and glycosylphosphatidylinositol (GPI)-anchored proteins: GPI-anchored proteins in liposomes and cells show similar behavior. Proc. Natl. Acad. Sci. USA **91:**12130–12134.
45. **Simons, K., and E. Ikonen.** 1997. Functional rafts in cell membranes. Nature **387:**569–572.
46. **Simons, K., and D. Toomre.** 2000. Lipid rafts and signal transduction. Nat. Rev. Mol. Cell Biol. **1:**31–39.
47. **Simpson, D. A., and R. A. Lamb.** 1992. Alterations to influenza virus hemagglutinin cytoplasmic tail modulate virus infectivity. J. Virol. **66:**790–803.
48. **Skehel, J. J., and D. C. Wiley.** 2000. Receptor binding and membrane fusion in virus entry: the influenza hemagglutinin. Annu. Rev. Biochem. **69:**531–569.
49. **Skibbens, J. E., M. G. Roth, and K. S. Matlin.** 1989. Differential extractability of influenza virus hemagglutinin during intracellular transport in polarized epithelial cells and nonpolar fibroblasts. J. Cell Biol. **108:**821–832.
50. **Steinhauer, D. A., S. A. Wharton, D. C. Wiley, and J. J. Skehel.** 1991. Deacylation of the hemagglutinin of influenza A/Aichi/2/68 has no effect on membrane fusion properties. Virology **184:**445–448.
51. **Takeda, M., G. P. Leser, C. J. Russell, and R. A. Lamb.** 2003. Influenza virus hemagglutinin concentrates in lipid raft microdomains for efficient viral fusion. Proc. Natl. Acad. Sci. USA **100:**14610–14617.
52. **Veit, M., E. Kretzschmar, K. Kuroda, W. Garten, M. F. Schmidt, H. D. Klenk, and R. Rott.** 1991. Site-specific mutagenesis identifies three cysteine residues in the cytoplasmic tail as acylation sites of influenza virus hemagglutinin. J. Virol. **65:**2491–2500.
53. **Vincent, S., D. Gerlier, and S. N. Manie.** 2000. Measles virus assembly within membrane rafts. J. Virol. **74:**9911–9915.
54. **Weissenhorn, W., A. Dessen, S. C. Harrison, J. J. Skehel, and D. C. Wiley.** 1997. Atomic structure of the ectodomain from HIV-1 gp41. Nature **387:**426–430.
55. **White, J. M.** 1992. Membrane fusion. Science **258:**917–924.
56. **Wiley, D. C., and J. J. Skehel.** 1987. The structure and function of the hemagglutinin membrane glycoprotein of influenza virus. Annu. Rev. Biochem. **56:**365–394.
57. **Zhang, J., A. Pekosz, and R. A. Lamb.** 2000. Influenza virus assembly and lipid raft microdomains: a role for the cytoplasmic tails of the spike glycoproteins. J. Virol. **74:**4634–4644.
58. **Zürcher, T., G. Luo, and P. Palese.** 1994. Mutations at palmitylation sites of the influenza virus hemagglutinin affect virus formation. J. Virol. **68:**5748–5754.